A metamaterial absorber for the terahertz regime: Design, fabrication and characterization

Hu Tao[1†], Nathan I. Landy[2†], Christopher M. Bingham[2], Xin Zhang[1], Richard D. Averitt[3], and Willie J. Padilla[2]

[1]*Boston University, Department of Manufacturing Engineering, 15 Saint Mary's Street, Brookline, Massachusetts 02446, USA.*
[2]*Boston College, Department of Physics, 140 Commonwealth Ave., Chestnut Hill, MA 02467 USA.*
[3]*Boston University, Department of Physics, 590 Commonwealth Avenue, Boston, Massachusetts 02215, USA.*
[†] *Contributed equally to this work.*
Willie.Padilla@bc.edu

Abstract: We present a metamaterial that acts as a strongly resonant absorber at terahertz frequencies. Our design consists of a bilayer unit cell which allows for maximization of the absorption through independent tuning of the electrical permittivity and magnetic permeability. An experimental absorptivity of 70% at 1.3 terahertz is demonstrated. We utilize only a single unit cell in the propagation direction, thus achieving an absorption coefficient α = 2000 cm^{-1}. These metamaterials are promising candidates as absorbing elements for thermally based THz imaging, due to their relatively low volume, low density, and narrow band response.

OCIS codes: (40.2235)Far infrared or Terahertz; (50.6624) Subwavelength structures; (110.6795) Terahertz Imaging; (160.1890) Detector Materials; (160.3918) Metamaterials; (260.5740) Resonance.

References and links

1. G. P. Williams, "Filling the THz gap - high power sources and applications," Rep. Prog. Phy. **69,** 301–326 (2006).
2. M. Tonouchi, "Cutting-edge terahertz technology," Nat. Photonics **1,** 97–105 (2007).
3. X.-C. Zhang, "Terahertz wave imaging: horizons and hurdles," Phys. Med. Biol. **47,** 3667–3677 (2002).
4. T. W. Crowe, T. Globus, D. L. Woolard and J. L. Hesler, "Terahertz sources and detectors and their application to biological sensing," Philosophical Transactions of the Royal Society of London A **362,** 265–377 (2004).
5. F. Oliveira, R. Barat, B. Schulkin, F. Huang, J. Federici and D. Gary, "Neural network analysis of terahertz spectra of explosives and bio-agents," Proc. SPIE **5070,** 60–70 (2003).
6. D. Zimdars, "Fiber-pigtailed terahertz time-domain spectroscopy instrumentation for package inspection and security imaging," Proc. SPIE **5070,** 108–116 (2003).
7. J. F. Federici, B. Schulkin, F. Huang, D. Gary, R. Barat, F. Oliveira and D. Zimdars, "THz imaging and sensing for security applications - explosives, weapons, and drugs," Semicond. Sci. Technol. **20,** S266–S280 (2005).
8. H.-B. Liu, Y. Chen, G. J. Bastiaans and X.-C. Zhang, "Detection and identification of explosive RDX by THz diffuse reflection spectroscopy," Opt. Express **11,** 2549–2554 (2003).
9. J. Barber, D. E. Hooks, D. J. Funk and R. D. Averitt, A. J. Taylor and D. Babikov, "Temperature-dependent far-infrared spectra of single crystals of high explosives using terahertz time-domain spectroscopy," J. Phys. Chem. A **109,** 3501–3505 (2005).
10. W. J. Padilla, M. T. Aronsson, C. Highstrete, M. Lee, A. J. Taylor and R. D. Averitt, "Electrically resonant terahertz metamaterials: theoretical and experimental investigations," Phys. Rev. B **75,** 041102R (2007).
11. T. J. Yen, W. J. Padilla, N. Fang, D. C. Vier, D. R. Smith, J. B. Pendry, D. N. Basov and X. Zhang, "Terahertz Magnetic Response from Artificial materials," Science **303,** 1494–1496 (2004).

#93760 - $15.00 USD Received 12 Mar 2008; revised 25 Apr 2008; accepted 29 Apr 2008; published 2 May 2008

12. H-T Chen, W. J. Padilla, J. M. O. Zide, A. C. Gossard, A. J. Taylor and R. D. Averitt, "Active Metamaterial Devices," Nature **444,** 597–600 (2006).
13. W. J. Padilla, A. J. Taylor, C. Highstrete, Mark Lee and R. D. Averitt, "Dynamical electric and magnetic metamaterial response at terahertz frequencies," Phys. Rev. Lett. **96,** 107401 (2006).
14. D. R. Smith, W. J. Padilla, D. C. Vier, S. C. Nemat-Nasser and S. Schultz, "A composite medium with simultaneously negative permeability and permitivity," Phys. Rev. Lett. **84,** 4184–4187 (2000).
15. R. A. Shelby, D. R. Smith and S. Schultz, "Experimental verification of a negative index of refraction," Science **292,** 77–79 (2001).
16. J. B. Pendry, "Negative refraction makes a perfect lens," Phys. Rev. Lett. **86,** 3996 (2000).
17. J. B. Pendry, D. Schurig and D. R. Smith, "Controlling Electromagnetic Fields," Science **312,** 1780–1782 (2006).
18. D. Schurig, J. J. Mock, B. J. Justice, S. A. Cummer, J. B. Pendry, A. F. Starr and D. R. Smith, "Metamaterial Electromagnetic Cloak at Microwave Frequencies," Science **314,** 977–980 (2006).
19. N. I. Landy, S. Sajuyigbe, J. J. Mock, D. R. Smith and W. J. Padilla, "A Perfect Metamaterial Absorber," Submitted to Phys. Rev. Lett.
20. D. Schurig, J. J. Mock and D. R. Smith, "Electric-field-coupled resonators for negative permittivity metamaterials," Appl. Phys. Lett. **88,** 041109 (2006).
21. D. R. Smith, S. Schultz, P. Markos and C. M. Soukoulis, "Determination of effective permittivity and permeability of metamaterials from reflection and transmission coefficients," Phys. Rev. B **65,** 195104 (2001).
22. G. Dolling, M. Wegener, C. M. Soukoulis and S. Linden, "Negative-index metamaterial at 780 nm wavelength," Opt. Lett. **32,** 53–55 (2007).
23. F. Cremer, P. B. W. Schwering, W. Jong, K. Scutte and A. N. Jong, "Infrared polarization measurements of targets and background marine environment," Proc. SPIE **4370,** 169–179 (2001).
24. F. A. Sadjadi and C. L. Chun, "Automatic detection of small objects from infrared state-of-polarization," Opt. Lett. **28,** 531–533 (2003).
25. T. White, N. Butler and R. Murphy, "An uncooled IR sensor with a digital focal plane array," IEEE Eng. Med. Biol. Mag. **17,** 60–65 (1998).
26. J. Wauters, "Doped silicon creates new bolometer material," Laser Focus World **33,** 145–149 (1997).
27. M. Almasri, D. P. Butler and Z. Celik-Butler, "Self-supporting uncooled infrared bolometers with low thermal mass," J. Microelectromechanical Syst. **10,** 469–476 (2001).
28. H. K. Lee, J. B. Yoon, E. Yoon, S. B. Ju, Y. J. Wong, W. Lee and S. G. Kim, "A high fill-factor infrared bolometer using micromachined multilevel electrothermal structures," IEEE Trans. Electron. Devices **46,** 1489–1491 (1999).
29. L. Baorino, E. Monticone, G. Amato, R. Steni, G. Benedetto, A. M. Rossi, V. Lacquaniti, R. Spagnolo, V. Lysenko and A. Dittmar, "Design and fabrication of metal bolometers on high porosity silicon layers," Microelectron. J. **30,** 1149–1154 (1999).
30. D. M. Mittleman, M. Gupta, R. Neelamani, R. G. Baraniuk, J. V. Rudd and M. Koch, "Recent advances in terahertz imaging," Appl. Phys. Lett. B **68,** 1085–1094 (1999).
31. S. Nishizawa and K. Sakai, T. Hangyo, T. Nagashima, M. W. Takeda, K. Tominaga, A. Oka, K. Tanaka and O. Morikawa, "Terahertz time-domain spectroscopy," Terahertz Optoelectronics **97,** 203–269 (2005).
32. A. W. M. Lee and Q. Hu, "Real-time, continuous-wave imaging by use of a microbolometer focal-plane array," Opt. Lett. **30,** 2563–2565 (2005).
33. H.-T. Chen, J. F. O'Hara, A. K. Azad, A.J. Taylor, R. D. Averitt, D. B. Shrekenhamer, and W. J. Padilla, "Experimental Demonstration of Frequency Agile Terahertz Metamaterials," Nat. Photonics, in press.

The electromagnetic response of natural materials forms the basis for the construction of most modern optoelectronic devices. However, this EM response is not evenly distributed across the electromagnetic spectrum. At frequencies of a few hundred gigahertz and lower, electrons are the principle particles which serve as the workhorse of devices. On the other hand, at infrared through optical / UV wavelengths, the photon is the fundamental particle of choice. In-between these two fundamental response regimes there exists a region comparatively devoid of material response, commonly referred to as the "terahertz gap" (0.1-10 THz, λ=3mm-30μm) [1, 2]. Although enormous efforts have focused on the search for "terahertz" materials or alternative novel techniques to enable the construction of device components, much work remains. There is a wide range of natural phenomena that could be probed with terahertz (THz) devices. Specifically, a THz detector would be useful for imaging in areas such as biology [3, 4] and security [5, 6, 7, 8, 9].

Recently, there has been considerable effort to construct engineered electromagnetic materials for operation specifically within the void of natural material response described above

#93760 - $15.00 USD Received 12 Mar 2008; revised 25 Apr 2008; accepted 29 Apr 2008; published 2 May 2008

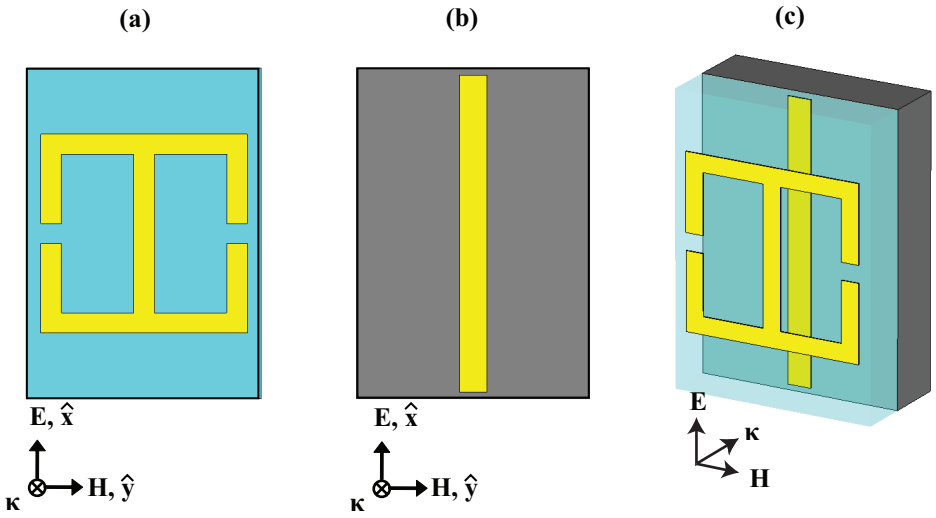

Fig. 1. (color) Schematics of the THz absorber: (a) electric resonator on the top of a polyimide spacer; (b) cut wire on GaAs wafer; (c) single unit cell showing the direction of propagation of incident EM wave. The unit cell is 34 μm wide and 50 μm in length. The line width and gap of the electric resonator is 3 μm. The side length of the square electric resonator is 30 μm, the side length of the cut wire is 48 μm, and the width of the cut wire is 4 μm. Thickness of the electric resonant ring and cut wire is 200 nm. The spacer of polyimide is 8 μm thick, and the GaAs wafer is 500 μm thick.

[10, 11, 12, 13]. These artificial systems, called metamaterials (MMs), are composites whose EM properties originate from oscillating electrons in unit cells comprised of highly conductive and shaped metals such as gold or copper. The sub-wavelength unit cell is replicated to form a material, which allows for a designed resonant response of the metamaterial's electrical and magnetic properties. Metamaterials can be regarded as effective media and characterized by a complex electric permittivity $\widetilde{\varepsilon}(\omega) = \varepsilon_1(\omega) + i\varepsilon_2(\omega)$ and complex magnetic permeability $\widetilde{\mu}(\omega) = \mu_1(\omega) + i\mu_2(\omega)$. Resonant structures that couple strongly to either the electric [10] or magnetic [11] fields have been demonstrated at terahertz. Significant growth in metamaterial research has been due to efforts to create negative refractive index (NRI) materials [14, 15, 16] and, more recently, invisibility cloaks [17, 18]. As such, the primary focus has been on the index of refraction defined as $\widetilde{n}(\omega) = \sqrt{\widetilde{\varepsilon}(\omega)\widetilde{\mu}(\omega)} = n_1 + in_2$, where one desires $n_1 < 0$ for negative index or $0 < n_1 < 1$ for cloaks. To create such structures, it is important to minimize losses over the operating frequency range, which is associated with the imaginary portion of the index, and thus strive for $n_2 \to 0$. Conversely, for many other applications it would be desirable to maximize the metamaterial loss which is an aspect of metamaterial research that, to date, has received very little attention. A recent example is the creation of a resonant high absorber which has been demonstrated at microwave frequencies [19]. Such an absorber would be of particular importance at terahertz frequencies where it is difficult to find naturally occurring materials with strong absorption coefficients that are also compatible with standard microfabrication techniques. By fabricating bilayer metamaterial structures it becomes possible to simultaneously tune $\widetilde{\varepsilon}(\omega)$ and $\widetilde{\mu}(\omega)$ such that a high absorptivity can be achieved. In principle, this tunability could lead to near unity absorptivity. In practice this is limited by achievable fabrication tolerances.

#93760 - $15.00 USD Received 12 Mar 2008; revised 25 Apr 2008; accepted 29 Apr 2008; published 2 May 2008

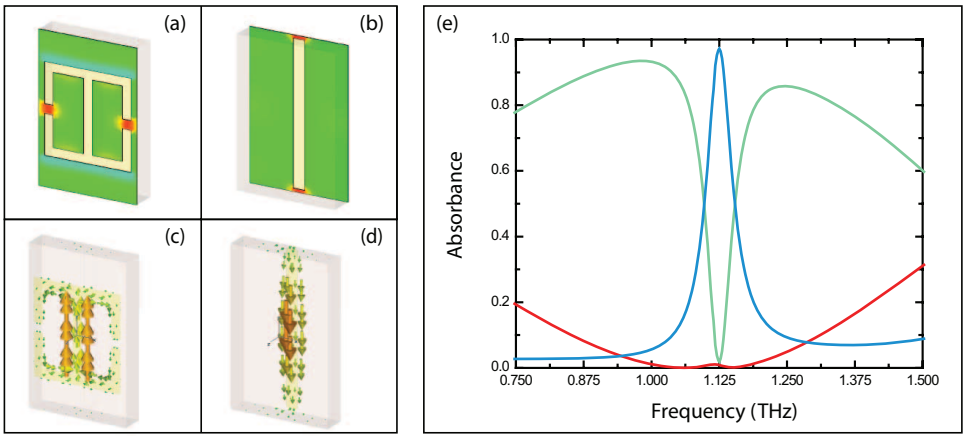

Fig. 2. (color) Simulation results for the electric resonator ring and cut wire. (a) and (b) show the x-component of the electric field of the electric resonator ring and cut wire at resonance, respectively; (c) and (d) show the anti-parallel currents driven by magnetic coupling. (e) The absorptivity (blue) yields a value of 98% at 1.12 THz. Reflection (green) and Transmission (red) are both at normal incidence.

We present a first generation terahertz metamaterial absorber which achieves a resonant absorptivity of 70% at 1.3 THz. Given the 6 μm thickness of our metamaterial, this corresponds to a power absorption coefficient of α =2000 cm^{-1} which is significant at THz frequencies. The strong absorption coefficient makes this low volume structure a promising candidate for the realization of enhanced, spectrally selective, thermal detectors. A single unit of the absorber consists of two distinct metallic elements: an electrical ring resonator (ERR) Fig. 1 (a) and a split wire Fig. 1 (b). The electrical ring resonator (ERR) consists of two single split rings sitting back to back. The two inductive loops are of opposite handedness and thus couple strongly to a uniform electric field, and negligibly to magnetic fields [10, 20]. The magnetic component of light couples to both the center section of the electric resonator and the cut wire, thus generating antiparallel currents resulting in resonant $\mu(\omega)$ response. The magnetic response can therefore be tuned independently of the electric resonator by changing the geometry of the cut wire and the distance between elements. By tuning each of the resonances it is possible to approximately match the impedance ($Z = \sqrt{\mu/\varepsilon}$) to free space, i.e. ($\varepsilon = \mu$) $\Rightarrow$ ($Z = Z_0$) and minimize the reflectance at a specific frequency. When the material is impedance-matched, the transmission[21] is governed by the quantity $n_2 kd$, which can be simultaneously tuned with Z to obtain high absorption.

Computer simulations were performed using the commercial finite-difference time domain solver CST Microwave Studio ^{TM} 2006B and 2008. The metamaterials depicted in Fig. 1 were modeled as lossy gold with a conductivity of $\sigma = 1.0\times10^7$ S/m. The bottom substrate was modeled as gallium arsenide with a dielectric constant of 10.75. A 8 μm thick layer of dielectric, $\widetilde{\varepsilon}$=3.5+i0.02 was used as the spacer between the two metallic metamaterial elements. We first investigated the S-parameters of transmission ($\widetilde{S}_{21}$) and reflection ($\widetilde{S}_{11}$) of a single unit cell with Perfect Electric (PE) and Perfect Magnetic (PM) boundary conditions along the $\hat{x}$ and $\hat{y}$ directions, respectively, (see Fig. 1). The absorptivity was calculated using the equation $A = 1 - |S_{21}|^2 - |S_{11}|^2$. The electric and magnetic fields were examined at resonance to verify that we were coupling to the correct resonant mode of each metamaterial element. In Fig. 2, the resonant component of the electric field at resonance is plotted for the electric ring resonator (ERR) (a)

#93760 - $15.00 USD Received 12 Mar 2008; revised 25 Apr 2008; accepted 29 Apr 2008; published 2 May 2008

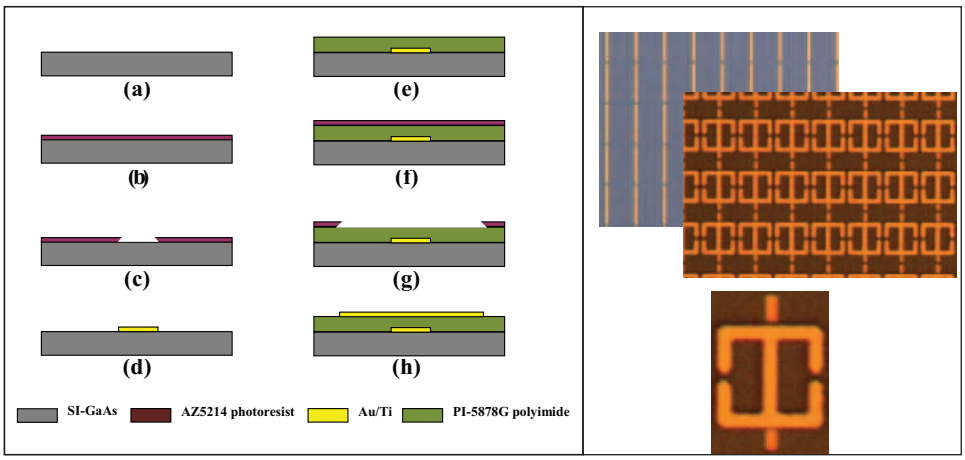

Fig. 3. (color) Left panel describes the development process for fabrication of the terahertz absorber. Right panel shows photographs of the split wire (top) electric ring resonator and split wire (middle) and an individual unit cell of the terahertz absorber (bottom).

and the split wire (b). The electric field is concentrated strongly in the gaps of the ring resonator and at the edges of the split wire in accord with previous results [10, 20]. Figures 2 (c) and (d) show a vector plot of the surface current density for the ERR and the split wire, respectively. Notice that at resonance currents are anti-parallel in the two metamaterial elements, which is the basis of the magnetic response and consistent with previous results [19, 22].

By changing the electric and magnetic resonances individually, we were able to create a condition such that the material was at an impedance near the free space value in a region of very low T(ω). The simulated transmission is relatively low across the entire range shown in Fig. 2 (e), whereas the reflectivity is relatively high except near the resonance at 1.12 THz where it drops to a value of 2%. Near unity absorbtion is theoretically possible and here we achieve a simulated value of 98% at 1.12 THz, as shown in Fig. 2(e). It should be noted that at THz frequencies the magnetic response of both natural materials and metamaterials is significantly weaker than the electric. Thus, matching the exact form of the $\varepsilon(\omega)$ and $\mu(\omega)$ resonances becomes increasingly difficult at these and higher frequencies. Further, from a viewpoint of spectrally selective thermal imaging, it is desirable to have a narrow-band absorber. Thus we strive for two requirements of our metamaterials at our target frequency, i.e. $Z = Z_0$ so that $R = 0$ and $n_2 kd \gg 0$ so that $T \rightarrow 0$. With these two goals we can achieve a significant and narrow-band $A(\omega)$, but tolerance limits associated with microfabrication can reduce the absorptivity from unity.

We fabricated the metamaterial shown in Fig. 1 using a surface micromachining process, as shown in Fig. 3. A semi-insulating GaAs wafer was chosen because it is highly transmissive at THz frequencies. AZ5214e image reversal photoresist was spin-coated and patterned using standard photolithography. A 200 nm-thick Au/Ti film was E-beam evaporated to create the cut wire on the bottom layer. Lift off of the photoresist was achieved by rinsing in acetone for several minutes. The liquid polyimide, HD Microsystems ^{TM} PI-5878G, was spin-coated at 2,000 rpm on the GaAs wafer to form an insulating spacer with a thickness of 8 μm, and cured for five hours in an oven at 275 °C in a nitrogen environment after the soft bake at 110 °C for 6 minutes on a hot plate. AZ5214e image reversal photoresist was spin-coated, aligned, and patterned using standard photolithography. Another 200 nm-thick Au/Ti was E-beam evaporated

#93760 - $15.00 USD Received 12 Mar 2008; revised 25 Apr 2008; accepted 29 Apr 2008; published 2 May 2008

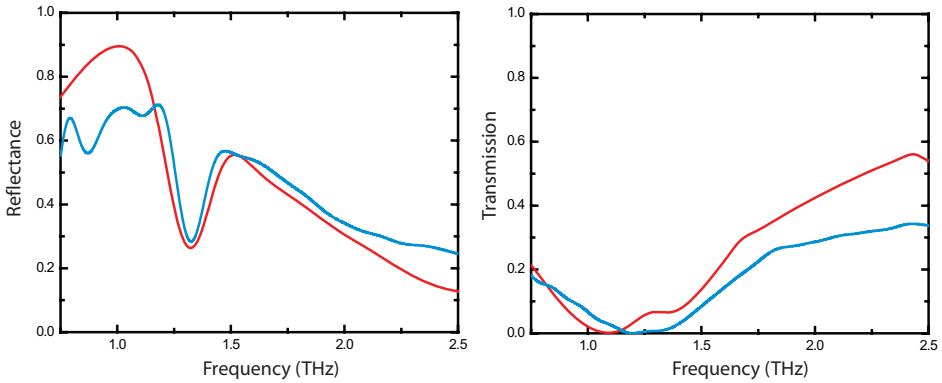

Fig. 4. (color) Experimental results showing the transmission intensity and reflection intensity. The blue lines are experiment and the red line the simulations. The reflectance measurement was performed at 30° off-normal. The transmission measurement was performed at normal incidence.

as the material of the electric resonant ring on the top layer and then lifted off. Microscopic images of the as-fabricated samples are shown in Fig. 3 (right).

We experimentally verified the behavior of the absorber by measuring the transmission and reflectance of a large (1 cm$\times$1 cm) planar array. We used an evacuated Fourier transform infrared (FTIR) spectrometer in the range from 300 GHz - 3 THz (10 - 100 cm $^{-1}$) with 15 GHz (0.5 cm^{-1}) spectral resolution. For transmission measurements the sample was mounted in the FTIR at normal incidence with the electric field perpendicular to the gap of ERR, as depicted in Fig. 1(a). Reflection was performed at an angle of 30° due to experimental limitations. The blue curves in Figs. 4(a) and (b) show, respectively, the measured reflectivity and transmission. Measured R(ω) and T(ω) differ significantly from that simulated as shown in Fig. 2(e). However, it should be noted that values used in simulation for the polyimide spacing layer were estimated based on published values at lower GHz frequencies. Further, the thickness of the polyimide layer was measured to be closer to 6μm rather than the 8μm used in simulations. Taking both of these factors into account, we are able to match measurements using an experimentally determined value for polyimide of $\varepsilon = 2.5 + i0.2$. The red curves are the corresponding simulations which are in good agreement with experiment. The simulated reflectance matches reasonably well near the resonance with slight deviations at lower and higher frequencies. The simulated transmission also agrees well with experiment, particularly in the vicinity of the resonance. Further, the simulated T(ω) reproduces the same qualitative features as experiment, including a distinct kink near 1.75 THz.

From experimental data presented in Fig. 4, the corresponding absorptivity is determined as shown in Fig. 5. These results demonstrate that the as-fabricated MMs have a strong resonance at around 1.3 THz and a high absorptivity of approximately 70%. Simulations show good agreement with experiment (red). The simulated absorptivity at resonance matches very well with the measured value. The off-resonance absorptivity is higher in experiment than in simulation due to differences in the experimental and simulated S-parameters. The response of absorber could be further improved through refinement and optimization of the fabrication process.

The absorber presented in this work absorbs strongly for light polarized along the $\hat{x}$ direction, as shown in Fig. 1, but poor for $\hat{y}$ polarized light, as shown in Fig. 6. In this polariza-

#93760 - $15.00 USD Received 12 Mar 2008; revised 25 Apr 2008; accepted 29 Apr 2008; published 2 May 2008

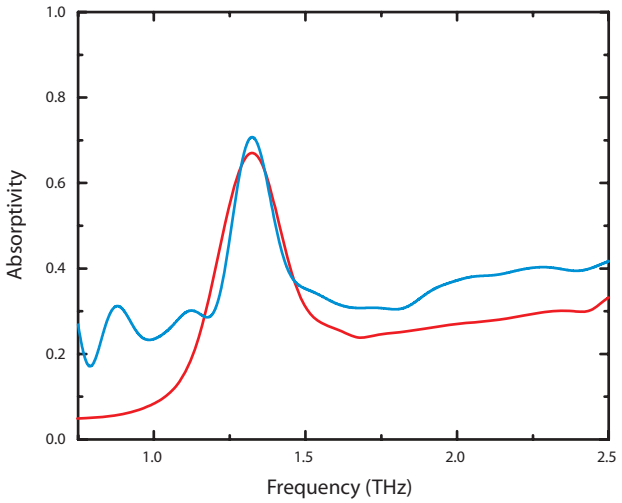

Fig. 5. (color) Experimental results showing absorptivity. Experimental results are in blue and simulation is in red. The experimental absorptivity reaches a maximum value of 70% at 1.3 THz. The simulated absorptivity reaches a value of 68% at the same frequency.

tion, the electric field is perpendicular to the center stalk of ERR, so an electric response cannot be driven. Similarly, there are no parallel wires for the magnetic field to develop a flux through and thus no net magnetic response. Such a polarization-sensitive device is desirable for both mm-wave and THz imaging as reflections from metallic objects often saturate the imager, thus significantly degrading it performance, in a problem known as "glint". Additionally, polarization-sensitive detection has been shown to aid in discrimination of objects in a scene [23, 24]. However, by incorporating higher symmetry metamaterials, (similar to those presented here), a polarization-insensitive design could be acheived.

The performance of a THz radiation detector depends on the efficiency of converting radiation energy to an output signal. Therefore, maximizing the THz radiation absorption efficiency is integral to the development of a functional THz detector/imager. It is difficult to find strongly absorbing materials at THz frequencies that are compatible with standard photolithography. Thus, a potential application of these metamaterial structures is as the absorbing elements in thermal detectors. A strong absorption coefficient is also necessary to have a small thermal mass. This is important for optimizing the temporal response of thermal detectors. The metamaterial presented here has a 6 micron thick film and 70% absorptivity, which yields an absorption coefficient of 2000 cm^{-1}. With better fabrication tolerances we could approach the simulated results (Fig. 2). This would yield an absorption coefficient three times greater than experimentally demonstrated here.

Many micro thermal detectors (typically based on bolometric detection and appropriately termed microbolometers) utilize several materials as the sensing element such as VOx [25], poly-Si-Ge [26], YBCO [27], or metal resistors such as, titanium [28] and niobium [29]. Some of these materials are not fully compatible with microfabrication processing. For those that are, however, it is difficult and thus expensive to prepare or deposit a high quality film. Additionally, most of these materials show broad-band absorption. This limits potential applications, such as spectroscopic detection of explosive materials, which show unique responses at var-

#93760 - $15.00 USD Received 12 Mar 2008; revised 25 Apr 2008; accepted 29 Apr 2008; published 2 May 2008

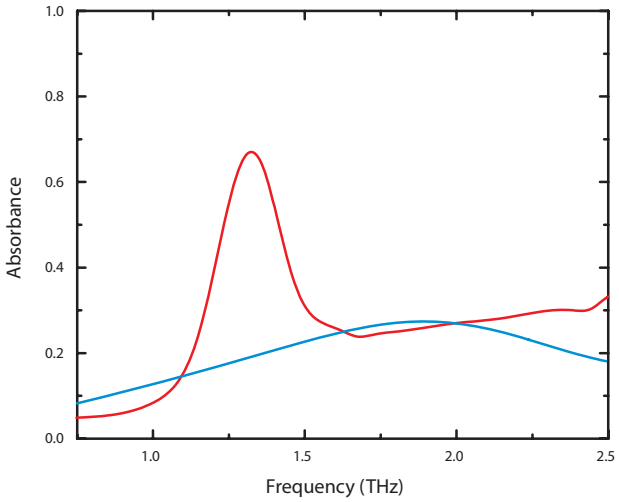

Fig. 6. (color) Simulation results comparing absorptivity for both polarizations. When the electric field is polarized parallel to the center stalk of the ERR (red) absorption reaches 70%. In the opposite polarization, the absorption only reaches 27%

ied frequencies [9]. The narrowband absorptivity of metamaterials presented here, on the other hand, enable spectrally selective detection. Furthermore, MMs are geometrically scalable and have been demonstrated over many decades of frequency. Thus, our results are not limited to terahertz frequencies and may be used over much of the electromagnetic spectrum. Another salient feature of the design presented here is that it may be combined with semiconducting materials or ferroelectrics to enable optically or electrically tunable frequency agile terahertz metamaterials. This would further permit a hyperspectral metamaterial focal plane array imager able to imaging over a relatively large band [33]. Planar metamaterial absorbers consisting of different unit cells with distinct resonance frequencies may permit "multi-color" imaging.

In summary, we have demonstrated that the electromagnetic response of metamaterials can be tailored by manipulating the geometries of electric and magnetic resonators individually to create a highly selective absorber over a narrow band at THz frequencies. The successful demonstration of the high absorber holds great promise for future applications which includes metamaterial-based structures for creating a narrow-band, low thermal mass absorber as required for thermal sensing applications.

Acknowledgment

NIL, CMB, RDA and WJP acknowledge support from the Los Alamos National Laboratory LDRD program. This project has been supported in part by the DOD/Army Research Laboratory through grant W911NF-06-2-0040, DOE Los Alamos National Laboratory subcontract 50332-001-07 and DOE Los Alamos National Laboratory subcontract 50335-001-07. The authors would like to thank the Photonics Center at Boston University for technical support throughout the course of this research.

#93760 - $15.00 USD Received 12 Mar 2008; revised 25 Apr 2008; accepted 29 Apr 2008; published 2 May 2008

射 频 和 天 线 设 计 培 训 课 程 推 荐

易迪拓培训(www.edatop.com)由数名来自于研发第一线的资深工程师发起成立，致力并专注于微波、射频、天线设计研发人才的培养；我们于 2006 年整合合并微波 EDA 网(www.mweda.com)，现已发展成为国内最大的微波射频和天线设计人才培养基地，成功推出多套微波射频以及天线设计经典培训课程和 ADS、HFSS 等专业软件使用培训课程，广受客户好评；并先后与人民邮电出版社、电子工业出版社合作出版了多本专业图书，帮助数万名工程师提升了专业技术能力。客户遍布中兴通讯、研通高频、埃威航电、国人通信等多家国内知名公司，以及台湾工业技术研究院、永业科技、全一电子等多家台湾地区企业。

易迪拓培训课程列表：http://www.edatop.com/peixun/rfe/129.html

射频工程师养成培训课程套装

该套装精选了射频专业基础培训课程、射频仿真设计培训课程和射频电路测量培训课程三个类别共 30 门视频培训课程和 3 本图书教材；旨在引领学员全面学习一个射频工程师需要熟悉、理解和掌握的专业知识和研发设计能力。通过套装的学习，能够让学员完全达到和胜任一个合格的射频工程师的要求…

课程网址：http://www.edatop.com/peixun/rfe/110.html

ADS 学习培训课程套装

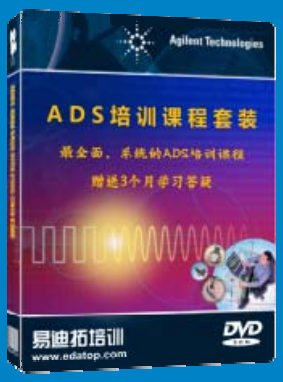

该套装是迄今国内最全面、最权威的 ADS 培训教程，共包含 10 门 ADS 学习培训课程。课程是由具有多年 ADS 使用经验的微波射频与通信系统设计领域资深专家讲解，并多结合设计实例，由浅入深、详细而又全面地讲解了 ADS 在微波射频电路设计、通信系统设计和电磁仿真设计方面的内容。能让您在最短的时间内学会使用 ADS，迅速提升个人技术能力，把 ADS 真正应用到实际研发工作中去，成为 ADS 设计专家...

课程网址： http://www.edatop.com/peixun/ads/13.html

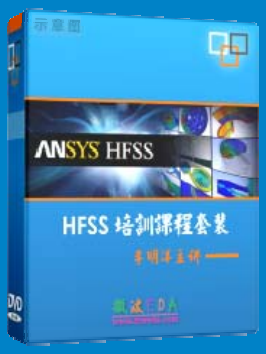

HFSS 学习培训课程套装

该套课程套装包含了本站全部 HFSS 培训课程，是迄今国内最全面、最专业的 HFSS 培训教程套装，可以帮助您从零开始，全面深入学习 HFSS 的各项功能和在多个方面的工程应用。购买套装，更可超值赠送 3 个月免费学习答疑，随时解答您学习过程中遇到的棘手问题，让您的 HFSS 学习更加轻松顺畅…

课程网址：http://www.edatop.com/peixun/hfss/11.html

CST 学习培训课程套装

该培训套装由易迪拓培训联合微波 EDA 网共同推出，是最全面、系统、专业的 CST 微波工作室培训课程套装，所有课程都由经验丰富的专家授课，视频教学，可以帮助您从零开始，全面系统地学习 CST 微波工作的各项功能及其在微波射频、天线设计等领域的设计应用。且购买该套装，还可超值赠送 3 个月免费学习答疑…

课程网址：http://www.edatop.com/peixun/cst/24.html

HFSS 天线设计培训课程套装

套装包含 6 门视频课程和 1 本图书，课程从基础讲起，内容由浅入深，理论介绍和实际操作讲解相结合，全面系统的讲解了 HFSS 天线设计的全过程。是国内最全面、最专业的 HFSS 天线设计课程，可以帮助您快速学习掌握如何使用 HFSS 设计天线，让天线设计不再难…

课程网址：http://www.edatop.com/peixun/hfss/122.html

13.56MHz NFC/RFID 线圈天线设计培训课程套装

套装包含 4 门视频培训课程，培训将 13.56MHz 线圈天线设计原理和仿真设计实践相结合，全面系统地讲解了 13.56MHz 线圈天线的工作原理、设计方法、设计考量以及使用 HFSS 和 CST 仿真分析线圈天线的具体操作，同时还介绍了 13.56MHz 线圈天线匹配电路的设计和调试。通过该套课程的学习，可以帮助您快速学习掌握 13.56MHz 线圈天线及其匹配电路的原理、设计和调试…

详情浏览：http://www.edatop.com/peixun/antenna/116.html

我们的课程优势：

※ 成立于 2004 年，10 多年丰富的行业经验，

※ 一直致力并专注于微波射频和天线设计工程师的培养，更了解该行业对人才的要求

※ 经验丰富的一线资深工程师讲授，结合实际工程案例，直观、实用、易学

联系我们：

※ 易迪拓培训官网：http://www.edatop.com

※ 微波 EDA 网：http://www.mweda.com

※ 官方淘宝店：http://shop36920890.taobao.com